



# System comprehensive risk assessment of urban rainstorm–induced flood-water pollution disasters

Shanqing Huang<sup>1,2,3</sup> · Huimin Wang<sup>1,2</sup> · Gaofeng Liu<sup>1</sup> · Jing Huang<sup>1</sup> · Jindi Zhu<sup>1</sup>

Received: 1 November 2022 / Accepted: 28 March 2023 / Published online: 4 April 2023  
© The Author(s), under exclusive licence to Springer-Verlag GmbH Germany, part of Springer Nature 2023

## Abstract

The urban rainstorm–induced flood-water pollution disaster is a kind of systematic risk, which may induce secondary disasters that can lead to more serious damage, so this paper first adopts the fuzzy comprehensive evaluation method to determine the flood risk by combining with the submergence depth derived from the risk field and other factors data, and then the grid environmental risk evaluation method, which is improved by increasing the induced possibility based on Bayesian theory, is used to evaluate the flood-induced water pollution risk, and the system comprehensive risk of rainstorm-induced flood-water pollution disasters is finally obtained by constructing risk level matrix, which can well depict the coupling superposition effect. Shenzhen City is selected as the study area, and the results showed that the area with high-risk of both flood and water pollution only accounts for about 0.14% of the total area, mainly distributed in the eastern junction of Longgang district and Pingshan district, where the rainstorms occur frequently and the enterprise risk sources are dense. The system comprehensive risk is mostly very low-low and very high-low, accounting for more than 76% of the total area. It is always necessary to pay attention not only to the areas with high risk level of both disasters, but also to the areas with high risk level of one disaster. The method proposed in this study can not only quantitatively reveal the formation of the induced risk, but also provide reference for early warning.

**Keywords** Urban · Induce · Flood · Water pollution · Risk field · System comprehensive risk

## Introduction

In recent years, the global warming and accelerated urbanization have affected the global climate, and the systemic risks caused by climate change are mainly concentrated in urban areas (Lian et al. 2017). Extreme heavy precipitation events occur frequently, and the intensity and frequency of rainstorms tend to increase, threatening social security, hindering economic development, damaging the ecological environment, and even causing serious casualties and

property losses, resulting in serious urban flood disasters that have attracted widespread attention (Chen et al. 2015; Jiang et al. 2018). Moreover, with the rapid development of the city and the deepening of industrialization, the surrounding area of the urban water sources is gradually occupied by some industrial enterprises, and sudden environmental events may occur due to natural disasters such as flood or human factors; pollutants will enter the water environment and flow along the water system, eventually affect the safety of water sources, thereby causing the safety of urban drinking water, and even leading to the stable development of society (Albanese et al. 2014; Boenne et al. 2014; Cozzani et al. 2010, Khakzad and Van Gelder 2018). Urban rainstorm–induced flood-water pollution has a chain effect and magnifies the disaster results, which is also a regional multi-hazard system problem with the characteristics of complexity and systemic, regional, and serious consequences. Therefore, it is necessary to conduct a comprehensive analysis and research on the two kinds of disasters, flood and water pollution, and the correlation between them, so as to provide

Responsible Editor: Marcus Schulz

✉ Gaofeng Liu  
gaofengliu@hhu.edu.cn

<sup>1</sup> Institute of Management Science, Business School, Hohai University, Nanjing 211100, China

<sup>2</sup> State Key Laboratory of Hydrology Water Resources and Hydraulic Engineering, Nanjing 210098, China

<sup>3</sup> School of Economics and Management, Chuzhou University, Chuzhou 239000, China

a scientific basis for the implementation of urban disaster prevention and mitigation measures.

In highly urbanized areas, with dense population and wealth accumulation, natural disasters such as rainstorm can easily induce a series of secondary or derivative disasters, which transfer disaster losses and cause more serious damage (Krausmann and Cruz 2013; Krishnakumar et al. 2022; Zhang et al. 2022). For this induced relationship, many studies have used disaster chain, domino effect, cascade effect, coupling relationship, and trigger relationship to describe and analyze it (Antonioni et al. 2015; Cozzani et al. 2014; Wu et al. 2021). The risk analysis of urban rainstorm-induced flood-water pollution first needs to determine the regional flood risk caused by rainstorm (Muis et al. 2015). Over the past decades, the assessment of urban flood risk induced by rainstorm has attracted the attention of scholars, a series of researches have been carried out, and many important achievements have been achieved (Link et al. 2019). At present, the more commonly used flood risk assessment methods mainly include historical disaster analysis method (Benito et al. 2004; Zhao et al. 2019), index system method (Jato-Espino et al. 2019; Shadmehri Toosi et al. 2019), remote sensing image method (Li et al. 2016; Shao et al. 2021), and scenario simulation method (Chen et al. 2018; Sun et al. 2014). Each method has its advantages and disadvantages, and there are also many mature research practices (Yin et al. 2015). Generally, the evaluation method is selected according to the spatial scale of the evaluation, the completeness of the basic data, the timeliness of the analysis results, and the accuracy of the evaluation results. It can also be combined with multiple methods for comprehensive evaluation. After assessing the regional flood risk level, how to determine the triggering relationship is the key of the study to carry out subsequent research. The current relevant research assumes that the induced event occurs definitely; without considering the induced possibility, the induced mechanism is not clear enough (Krausmann et al. 2011). Water pollution disaster risk is a type of regional environmental risk. Through regional environmental risk assessment, it is possible to systematically identify “hot spots” and key issues with high water pollution risk and become a solution to deal with urban flood-induced sudden water pollution and environmental problems, so as to provide decision makers with more targeted environmental risk management measures (Cao et al. 2019). The common methods of environmental risk assessment include comprehensive index method (Guan et al. 2022; Huang et al. 2011; Tesfamariam and Sadiq 2006), fuzzy mathematical method (Han et al. 2015; Liu et al. 2014; Zhang et al. 2020b), and environmental risk field evaluation method (Cao et al. 2019; Xing et al. 2016; Zhou et al. 2020a, b). Different methods are applicable to different scenarios, and how to accurately characterize and evaluate the systematic risk of water pollution in urban areas

is one of the focuses of this study. Urban rainstorm-induced flood-water pollution is a high-impact and low-probability event, once it occurs, the coupling and superposition of flood and water pollution will expand the harmfulness of disasters and lead to more serious disaster consequences; in essence, it is a multi-hazard problem (Chen et al. 2016; Johnson et al. 2016). The research on multi-hazard risk assessment is mainly divided into two types: one is the superposition of multi-hazard risk, including the superposition of disaster-causing factors and risks, is mostly linear superposition, is lacking research on the interaction between disasters, and is not accurate enough (Gill and Malamud 2016; Kappes et al. 2012). The other is the coupling of multi-hazard risk; there are complex relationships among multiple disasters, such as occurrence time, impact scope, and coupling effect (Bevacqua et al. 2020). The current research still starts from examples, and specific risks are studied based on the coupling of hazard factors, which is highly subjective and lacks a universal model. Therefore, it is necessary to seek a comprehensive risk assessment method for multi-hazard.

The comprehensive risk of urban rainstorm-induced flood-water pollution is a nonlinear problem, which cannot be simply superimposed, and is a systemic risk problem. Urban rainstorm flood is difficult to predict and strongly uncertain, and the urban flood-induced water pollution is a dynamic process constantly changing and evolving. Urban areas are not only subject to the combined effects of rainstorm flood and flood-induced water pollution, but also pay attention to their induced relationship, and ignoring the relationship will lead to inaccurate results. Compared with other areas, the surface environment and ecological environment in the city are very complex, and the coupling and superposition effect among multiple disasters expands the hazards of disasters and has a huge impact on the people’s lives’ safety, socio-economic property, and ecological environment in the city. There is no report on the comprehensive study of urban systemic risk induced by rainstorm, but cities are the most prone to induce systemic risk. For systemic risk, single-hazard risk assessment methods are difficult to apply and cannot fully reflect the interaction and impact between multiple disasters; thus, there is an urgent need to seek a comprehensive risk assessment method for urban rainstorm flood-induced systemic risk. The paper draws on the field theory and information diffusion theory in physics and considers that the risk system of each disaster includes risk sources, risk receptors, and transmission channels; multi-source, multi-pathway, and multi-receptor are the characteristics and forms of systemic risk in urban areas. Based on the risk formation mechanism, a mathematical model analogous to “physical field” is used to quantitatively describe and analyze the relevant disaster risks after the information obtained from the risk sources and risk receptors, and a complete systematic risk assessment model of urban rainstorm-induced

flood-water pollution based on the chain-field combination is constructed, which can more accurately and comprehensively characterize the characteristics, triggering process, distribution of each disaster risk, and systematic risk, and is easy to make decisions and control.

In the paper, the method is applied to our study area, Shenzhen City, to determine the system comprehensive risk zoning of rainstorm-induced flood-water pollution. The rest of the paper is organized as follows: “**Study area and data**” describes the study area and data resources. “**Methodology**” explains the methodology in detail. The results of the study are presented in “**Results**” and discussed in “**Discussion**.” “**Conclusion**” summarizes this study.

## Study area and data

### Study area

Shenzhen City is a coastal city located in the southern Guangdong Province, adjacent to Hong Kong. The geographical range of the land area is between 113°43′ and 114°38′ east longitude and 22°24′ and 22°52′ north latitude; the total area is 1997.47 square kilometers (km<sup>2</sup>) with a zonal distribution. The terrain of the whole area is complex, most of which are low hills, with gentle plateaus in between, and the coastal plain in the west, forming a special terrain with high southeast and low northwest. The city has direct jurisdiction over nine districts and one new

area: Futian, Luohu, Yantian, Nanshan, Bao’an, Longgang, Longhua, Pingshan, and Guangming districts and Dapeng New Area, as shown in Fig. 1. Shenzhen is the window of China’s reform and opening-up, with a developed economy and dense population; by the end of 2020, the city’s gross domestic product (GDP) was 2767.024 billion yuan, and the permanent resident population reached 17.6338 million. Shenzhen has a subtropical monsoon climate with mild and pleasant climate and abundant rainfall; the annual average rainfall is 1935.8 mm, 85% of which is concentrated in the flood season from April to October, and the spatial distribution of precipitation is uneven, showing a decreasing trend from southeast to west. There are many rivers, with short channels, and there are 362 rivers with a drainage area larger than 1 km<sup>2</sup>; the average length is less than 4 km. In addition, there are 149 water storage reservoirs in Shenzhen, 29 of which are involved in the water supply.

In recent years, Shenzhen has been one of the cities with the most rainstorm and flood in China due to climate, geographical location, topography, heavy rainfall, and external tide (Hadipour et al. 2020). As a rapidly developing megacity, the unreasonable discharge has generally polluted water bodies; there are still water pollution risks such as “heavy end, light source,” and the management of water pollution risk sources still needs to be strengthened (Geng et al. 2022; Qiu et al. 2019). Therefore, the study of rainstorm-induced flood pollution system risk assessment is of great significance for regional development planning and emergency management in Shenzhen.

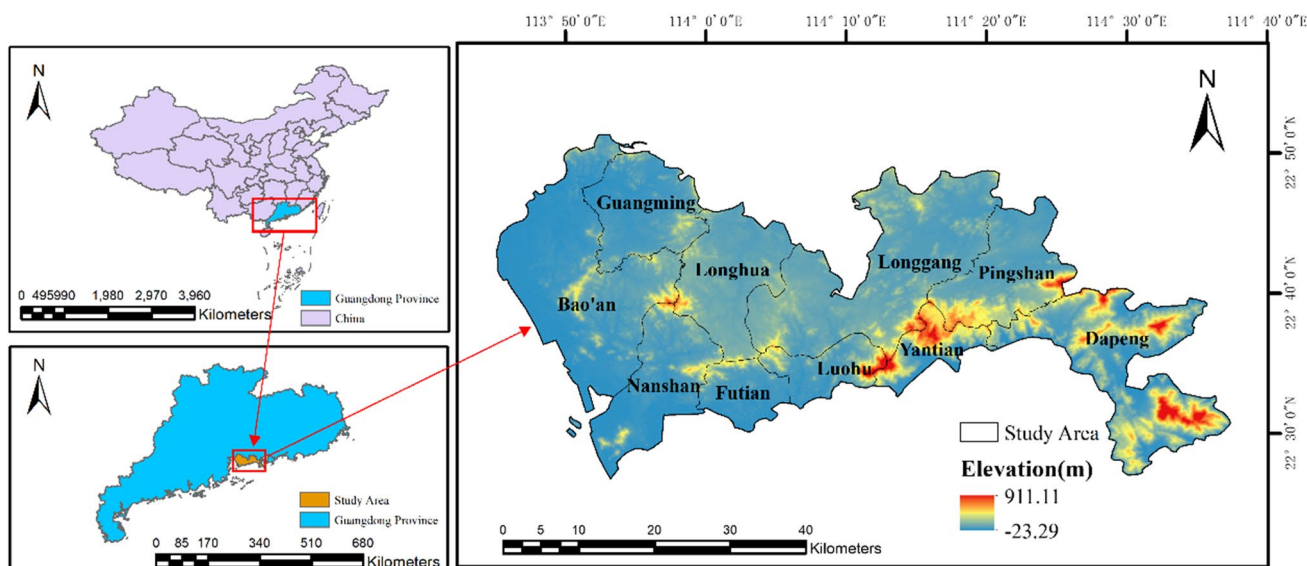


Fig. 1 Study area

## Data collection and preparation

### Flood data collection and preparation

The flood risk assessment method based on the index system has the advantages of easy data acquisition and simple modeling and has been widely used in urban flood risk assessment research (Shadmehri Toosi et al. 2019). In the paper, based on the regional disaster system theory and the natural disaster risk assessment principles, the urban flood risk evaluation index system is constructed by considering the flood risk influence factors from two aspects of disaster hazard and vulnerability (Arnell and Gosling 2016; Huang and Li 2021; Mukhopadhyay et al. 2016; Schumann and Andreadis 2016), which specifically includes four categories of 11 factor indicators, as shown in Table 1.

The multivariate heterogeneous flood factor data in the study area collected from different sources can be summarized into three categories:

1. Raster data. Digital elevation model (DEM) with 30-m resolution downloaded from the Geospatial Data Cloud (<http://www.gscloud.cn>) can extract elevation and slope and calculate the submergence depth by combining the idea of field. The land use type data with 30-m resolution come from the Ministry of Natural Resources GlobeLand30 2020 version (<http://www.globallandcover.com>), which determines the runoff coefficient.
2. Vector data. The administrative division data of the study area are from the Resource and Environmental Science and Data Center, Chinese Academy of Sciences (<http://www.resdc.cn>). The basic geographic data of rivers and road networks are from the database of the National Basic Geographic Information Center with a scale of 1:250,000 (<http://www.webmap.cn>).
3. Statistical data. The data of waterlogging points and waterlogging points water level needed for submergence depth are derived from waterlogging point measurement

stations of the Water Authority of Shenzhen Municipality. The GDP data are provided by the Shenzhen Statistical Yearbook, the population data are obtained from the Shenzhen Seventh National Census Bulletin, the spatial scale of the data is refined to the street, and not only the GDP per capita and GDP density can be obtained, but also the data on the distribution of the proportion of elderly people over 60 years old. The data on years of education are from the average education years of the population aged 15 and above in Shenzhen Seventh National Census Bulletin.

The study area is divided into 194,544 100 m × 100 m grid squares; the raw data is generalized into each grid cell by using Geographic Information System (GIS) spatial data analysis function; vector datasets are rasterized, and all datasets are spatialized and projected, resampled to 100 m × 100 m grid cells, cropped to the study area, and registered so that all input rasters accurately cover the same projection, cell size, and range.

### Water pollution data collection and preparation

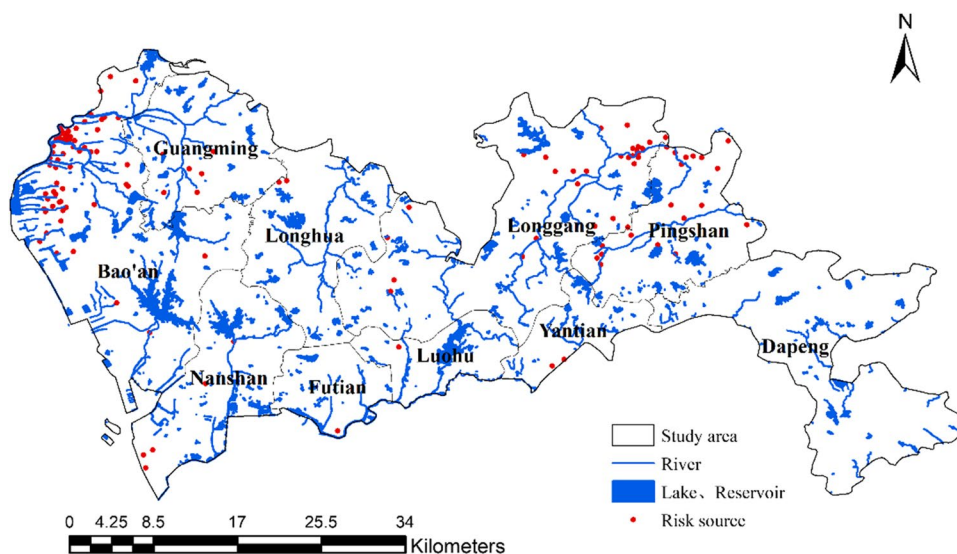
The collection and preparation of data related to water environmental risk assessment is carried out in terms of both risk source and risk receptor.

1. Risk source. Shenzhen has a wide range, and a venture enterprise can be regarded as a water environment risk source unit (Xing et al. 2016). In order to analyze the water environment pollution risk, the number and distribution of enterprises in Shenzhen, the key pollutant discharge enterprises of water environment in 2020, and the risk source level in the emergency plan of these enterprises are combined, and finally, 140 enterprises with overall higher risk level or above are finally determined as the risk sources for the water pollution study; the detailed location is shown in Fig. 2.

**Table 1** Urban flood risk evaluation index system

Criterion layer	Index layer	Scheme layer
Hazard	Disaster-causing factor	Submergence depth/mm
	Disaster-inducing environment	Elevation/m
		Slope (°)
		River network density (km/km <sup>2</sup> )
		Runoff coefficient
Vulnerability	Disaster-bearing body	Population density (people/km <sup>2</sup> )
		GDP density (ten thousand RMB/km <sup>2</sup> )
		The proportion of the elderly population/%
	Disaster prevention and mitigation capability	GDP per capita/ten thousand RMB
		Years of education/a
		Road network density (km/km <sup>2</sup> )

**Fig. 2** Distribution of water pollution risk sources in Shenzhen



The  $Q$  value reflecting the risk of each risk source itself, that is, the ratio of the maximum amount of environmental risk substances present to the critical amount (MEP 2018a), can be determined through statistical collation by comprehensively collecting the environmental protection information public announcements of each risk enterprise, the environmental statistics data of the Ecology Environment Bureau of Shenzhen Municipality, and the environmental risk assessment report and the emergency plan of each risk source enterprise, while each enterprise's production process and water environment risk control level  $M$  are obtained to characterize the flood prevention and control capability of the risk source. It should be noted that the  $Q$  value follows the principle of "equivalent hazard," which provides the possibility of superimposing risks later.

2. Risk receptor. Risk receptor data include water bodies such as lakes, reservoirs, and rivers and their water quality. The National Basic Geographic Information Center can also provide classification data of lakes and reservoirs with a scale of 1:250,000 (<http://www.web-map.cn>), combined with the previously obtained river data; their five grade distribution data can be obtained. The 2020 water quality monitoring cross-section data are from China Environmental Monitoring Station (<http://www.cnemc.cn>) and the 2020 Shenzhen Water Resources Bulletin, including the division of water quality functional zones and water quality monitoring data. In addition, historical sudden water pollution accident data are obtained from the Ecology Environment Bureau of Shenzhen Municipality and used to verify the results.

## Methodology

### Framework of research methods

This study constructs a systematic comprehensive risk assessment model of the integrated method of urban rainstorm-induced flood-water pollution by integrating methods and theories such as fuzzy comprehensive evaluation method, Bayesian network theory, and risk field theory and explore systematic risk assessment in urban areas (Fig. 3). Firstly, in the process of rainstorm-induced flood assessment, the influence factors and the flood risk process are uncertain and ambiguous; the fuzzy comprehensive evaluation method can solve these problems very well (Cai et al. 2019; Lai et al. 2020; Sarica et al. 2021; Zadeh 1965). How to obtain the submergence depth, which is a disaster-causing factor, is very important, and see "Rainstorm-induced submergence depth method." After collecting all factor data in Table 1 and referring to the research results of Huang and Li (2021) and Abdalla et al. (2014), the fuzzy comprehensive evaluation is used to assess urban rainstorm-induced flood risk in the study area; the specific process is shown in the left side of Fig. 3 and supplementary information. Secondly, it is necessary to determine whether and how likely an enterprise is at risk of water environment pollution. Bayesian network is used to quantitatively analyze the possibility of water environmental risks in enterprises from two perspectives: external risk threat and internal risk prevention capability. On this basis, the GIS spatial analysis method and regional growth method are introduced, and the factors such as water system flow direction, water system level, and water quality are comprehensively considered to carry out the water pollution environmental risk zoning study for the study area; the specific steps are shown in "Flood-induced water pollution risk

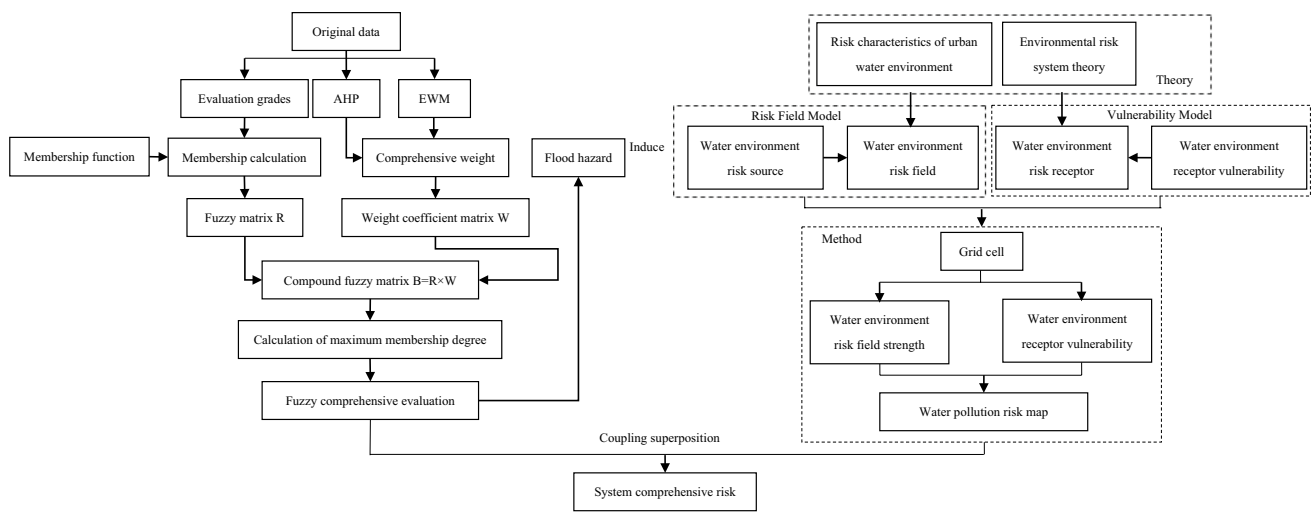


Fig. 3 Framework of the proposed method

assessment method.” Finally, the rainstorm-induced flood risk and the flood-induced water pollution risk are obtained from the above method; because the two risks are inconsistent in nature and correlated, it is necessary to find a coupling method (“Multi-hazard system comprehensive risk research”) to obtain the rainstorm-induced system risk in urban areas.

### Rainstorm-induced submergence depth method

This paper draws on the active submergence algorithm and uses the idea of risk field to construct an urban rainstorm submergence algorithm. The basic idea of the algorithm is that the rainstorms in local areas of the city cause water to accumulate in low-lying areas, which in turn overflows and spreads outward when the water is full, that is, submergence. All low-lying waterlogging points are risk sources, and the water level of the risk source is compared with the elevation of the adjacent outer ring grid to determine whether the ponding water spreads outward. This is the gradual submergence process of accumulated water along the terrain from high to low. In this process, it is also necessary to determine whether the ponding areas where multiple risk sources may spread have intersected (Huang et al. 2020; Zhang et al. 2020a). The specific steps of the algorithm are as follows:

1. Elevation attribute. Based on grid division 100 m×100 m, the DEM data is read to obtain the elevation value of each raster, which is marked and numbered by matrix (x, y) as the attribute value of DEM raster.
2. Determine the location of waterlogging points. These locations are the depressions prone to flood or obtained from actual surveys to further determine the raster number of risk sources and their waterlogging level, which are also used as DEM raster attributes.

3. Waterlogging diffusion. Starting from a waterlogging point risk source, the waterlogging diffusion is carried out in turn to judge whether the waterlogging level is greater than the elevation value of the eight grids in the adjacent outer circle. If it is more than, the waterlogging will spread to this grid, which has connectivity with the risk source, and the water depth value of the waterlogging point will be assigned to the grid waterlogging elevation. The flood spreads outward in a circle until the waterlogging level is less than the elevation value of the outer circle or reaches the boundary.
4. Repeat step (3) to get the diffusion range of all risk sources. When a grid participates in the diffusion of two or more nodes, its elevation each time is calculated as the original elevation.
5. Multi-risk source problem. After the diffusion of all risk sources is completed, it is judged whether there is a grid involved in the diffusion process of multiple risk source waterlogging point nodes. If there is, this grid is considered to be affected by the risk source with the highest waterlogging level, and the diffusion results in these grids are updated. Until all grids are judged, the diffusion is finished.
6. Submergence depth. Each grid waterlogging level minus its elevation value is the rainstorm submergence depth of the grid, and finally, the submergence result in the study area is obtained.

### Flood-induced water pollution risk assessment method

Urban flood is generally caused by short-term extreme heavy rainfall, which is sudden, and the discharge of enterprise risk substances induced by it is also sudden (Yang et al. 2018),

then the flood-induced water environment pollution disaster is a sudden environmental risk event. The environmental risk system consists of three elements: risk source, receptor, and pathway (Cao et al. 2019; Liu et al. 2018). The risk field can characterize the hazard mode and scale of enterprise risk sources, and the tolerance of risk receptors to hazard from risk sources can be characterized by receptor vulnerability (Cao et al. 2019; Zhou et al. 2020b). This paper refers to and revises the grid-based environmental risk analysis method in the Recommended Methods for Risk Assessment of Environmental Incidents in Administrative Areas (MEP 2018b) and combines the ideas and methods of the environmental risk field evaluation method to evaluate the flood-induced water pollution risk in the study area (Xing et al. 2016). This paper only conducts risk assessment for water environment pollution and assumes that the water environment pollutants leak instantaneously. The specific steps are as follows:

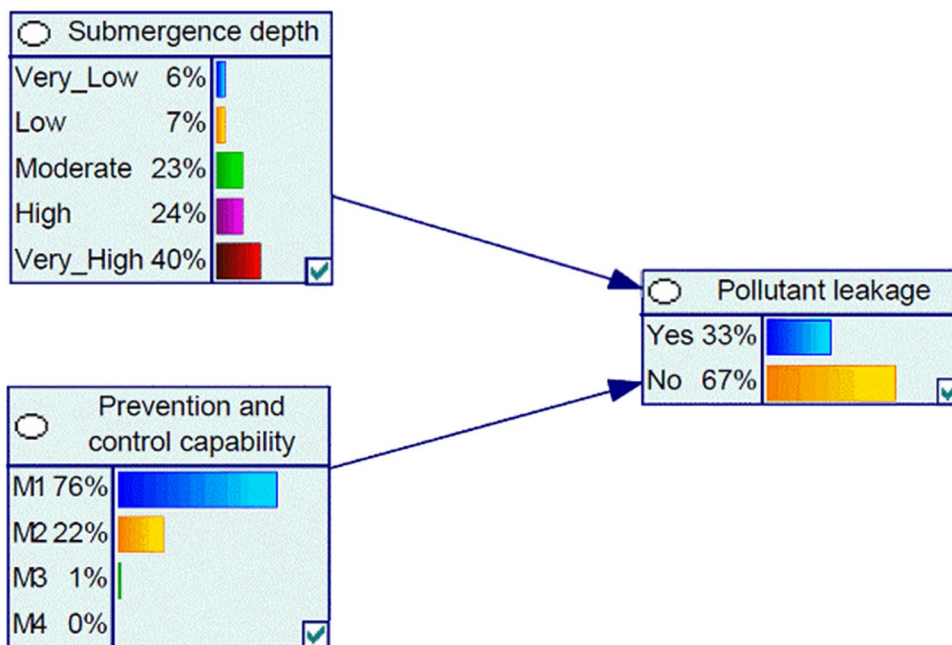
1. Grid division. Considering the size of the study area, the create fishnet function of ArcGIS is used to divide it into grids of 500 m × 500 m, which are marked and numbered with a matrix. The risk at (x, y) in the matrix is determined by the risk field strength and risk receptor vulnerability that may occur there.
2. Water environment risk field strength calculation. The strength of a grid water environmental risk field is related to the nature and amount of risk substances discharged and the distance between the grid and the risk source (Xing et al. 2016; Zhou et al. 2020a, b). The flood risk level is determined to quantify the impact of flood on the enterprise risk source, and then the grid-based environmental risk analysis method is introduced to cal-

culate the risk field strength of the water environmental risk source (Xing et al. 2016), which can be expressed as:

$$E_{x,y} = \begin{cases} \sum_{i=1}^n P_i Q_i P_{x,y}, & 0 \leq l_i \leq 2 \\ \sum_{i=1}^n (1 - \frac{l_i}{20}) P_i Q_i P_{x,y}, & 2 \leq l_i \leq 20 \\ 0, & 20 \leq l_i \end{cases} \quad (1)$$

where  $E_{x,y}$  is the flood-induced water environment risk field strength in a grid;  $Q_i$  is the ratio of the maximum amount of environmental risk substances present in the  $i$  th risk source to the critical amount;  $P_{x,y}$  is the probability of the risk field appearing in a certain grid, generally  $10^{-6}/a$ ;  $l_i$  is the distance between the grid center point and the risk source, the unit is km, and the maximum influence distance is set to 10 km;  $n$  is the risk source number;  $P_i$  is the occurrence probability of the flood-induced sudden water environmental events at risk sources (Alvarez-Galvez 2016; Khakzad and Gelder 2018). The risk itself is an uncertainty event, so the formation of environmental risk field also has a certain probability, that is, when the enterprise risk source is submerged, water environment pollution event will not necessarily occur. Whether the enterprise has risk material leakage, on the one hand, it should consider the submergence depth of the enterprise involved, and on the other hand, it is also related to the enterprise's own water environment risk prevention and control capabilities, thus calculating the possibility of the enterprise risk material leakage from the two perspectives of disaster-causing factors and prevention and control capabilities, as shown in Fig. 4.

Fig. 4 Bayesian network for the possibility of flood-induced water pollution



This conditional probability is mainly based on Bayes' theorem (Huang et al. 2021), which is determined by the following formula:

$$P_i = P(A_i/B) = \frac{P(A_i)P(B/A_i)}{\sum_{i=1}^n P(A_i)P(B/A_i)} \quad (2)$$

where  $P(A_i)P(B/A_i)$  is the total probability formula, which can deduce the probability value of the relevant states.  $B$  is the flood risk level,  $A_i$  refers to all the possible causes of event  $B$ ,  $P(A_i)$  refers to the prior probabilities derived from priori data, and  $i$  represents a specific variable.

The water pollution environmental risk field is affected by the external environment, the location of the risk sources, its own properties, and the propagation medium and is characterized by uneven intensity. The direction of water flow will flow from high to low and affect the surrounding grid only when the grid where the risk source is located is higher than the surrounding grid. In order to accurately determine the influence scope of the risk source, the regional growth method is introduced to search from the first circle grid closest to the risk source and compare the elevation value of the eight surrounding grids with those of the risk source (Zhou et al. 2020a, b). If it is less, this grid around the risk source is considered as the affected grid. Repeat the above steps and stop the search once the elevation value is greater than the last comparison grid value or the 10-km boundary is reached. Then, the risk field strength of each risk source in each grid is calculated according to formula (5). If the same grid is affected by multiple risk sources, the sum of the field strength of these risk sources on that grid is the risk field strength of that grid.

The flood-induced water environment risk field strength of each grid is standardized for comparison, and the formula is as follows:

$$E_{x,y} = \frac{E_{x,y} - E_{\min}}{E_{\max} - E_{\min}} \times 100 \quad (3)$$

where  $E_{x,y}$  is the flood-induced water environment risk field strength of a grid, multiplied by 100 to make all risk field strength fall within [1,100], so as to be consistent with the subsequent vulnerability;  $E_{\max}$  is the maximum water environment risk field strength in the whole area;  $E_{\min}$  is the minimum water environment risk field strength in the whole area

3. Water environmental risk receptor vulnerability calculation. Referring to the research results of Zhou et al. (2020a) and Cao et al. (2019), the sensitivities of different grids in the study area are determined mainly by considering the levels of rivers, lakes, and reservoirs and the functional area of water bodies. The method for

calculating the vulnerability of water environmental risk receptors is shown in Table 2.

4. Calculation of flood-induced water pollution risk index. The following formula (4) is used to calculate the flood-induced water pollution risk index in each grid:

$$R_{x,y} = \sqrt{E_{x,y} \times V_{x,y}} \quad (4)$$

where  $R_{x,y}$  is the flood-induced water pollution environmental risk index at  $(x, y)$ ;  $E_{x,y}$  is the flood-induced water environment risk field strength at  $(x, y)$ ;  $V_{x,y}$  is the vulnerability index of water environmental risk receptor at  $(x, y)$ . According to the grid environmental risk index value, the flood-induced water pollution risk is divided into four levels: very high risk ( $R_{x,y} > 80$ ), high risk ( $60 < R_{x,y} \leq 80$ ), moderate risk ( $30 < R_{x,y} \leq 60$ ), and low risk ( $R_{x,y} \leq 30$ ).

## Multi-hazard system comprehensive risk research

When multiple different types of risk sources act together on risk receptors, their physical hazard indicators should not be directly superimposed because their risk properties are different, and how to solve this problem has become a hot topic of research nowadays. In multi-hazard, linear stacking of all risks will result in inaccurate risk assessments due to the interaction between hazards (Andric and Lu 2016). However, different types of hazard interactions may affect disaster-bearing bodies simultaneously, leading to nonlinear additivity problems in risk assessment. After calculating the urban rainstorm-induced flood risk and flood-induced water pollution risk using the methods in the previous two sections, the [flood-pollution] risk level matrix (Table 3) is constructed from the two disaster risk level dimensions of flood and water pollution to acquire the urban rainstorm-induced flood-water pollution system comprehensive risk in each grid (Karatzetzou et al. 2021, 2022).

## Results

### Rainstorm-induced flood risk assessment

The short-time extreme heavy precipitation weather event in Shenzhen on April 11, 2019 is chosen to illustrate the application of the model. Under the influence of cold air and shear lines, short-time extreme heavy precipitation occurred from 19:00 to 23:00, accompanied by convective weather such as gusty winds and strong thunderstorms. The heavy rainfall was mainly distributed in Futian, Luohu, Bao'an, and Guangming districts, with heavy rainfall and short duration; the maximum average rainfall



**Table 2** Determination method of water environmental risk receptor vulnerability

Target	Index	Description	Weight	Score
Water environmental risk receptor vulnerability index	River, lake, reservoir grade	Grids through which grade 1 rivers, lakes, reservoirs, etc	1/3	100
		Grids through which grade 2 rivers, lakes, reservoirs, etc		80
		Grids through which grade 3 rivers, lakes, reservoirs, etc		60
		Grids through which grade 4 rivers, lakes, reservoirs, etc		40
		Grids through which grade 5 rivers, lakes, reservoirs, etc		20
	Water functional area	Grids through which class I water quality in rivers, lakes, reservoirs, etc	1/3	100
		Grids through which class II water quality in rivers, lakes, reservoirs, etc		80
		Grids through which class III water quality in rivers, lakes, reservoirs, etc		60
		Grids through which class IV water quality in rivers, lakes, reservoirs, etc		40
		Grids through which class V and inferior class V water quality in rivers, lakes, reservoirs, etc		20
	River, lake, reservoir buffer zone	Grids through which 1 km buffer zone of rivers, lakes, reservoirs, etc	1/3	100
		Grids through which 3 km buffer zone of rivers, lakes, reservoirs, etc		75
		Grids through which 5 km buffer zone of rivers, lakes, reservoirs, etc		50
		Grids through which 10 km buffer zone of rivers, lakes, reservoirs, etc		25

**Table 3** Comprehensive risk level matrix of flood–pollution

	Flood risk	Pollution risk		
		Low	Moderate	High
Very low	Very low-low	Very low-moderate	Very low-high	Very low-very high
Low	Low-low	Low-moderate	Low-high	Low-very high
Moderate	Moderate-low	Moderate-moderate	Moderate-high	Moderate-very high
High	High-low	High-moderate	High-high	High-very high
Very high	Very high-low	Very high-moderate	Very high-high	Very high-very high

is 65.5 mm in Luohu district, and more than half of the rainfall concentrated within 10 min, reaching 50- or 100-year return period, causing serious casualties and property damage. The hourly rainfall data from the rainfall monitoring stations on April 11, 2019 are interpolated to get the rainfall spatial distribution map in ArcGIS, and the water level of waterlogging points on that day is obtained from the waterlogging point measurement stations, as shown in Fig. 5.

The highest water level of the waterlogging point is in Futian district, followed by that in Bao’an district and Guangming district, which is not quite consistent with the

distribution of heavy precipitation because of the geographical location of the waterlogging point measurement stations, which has a strong relationship with rainstorm-induced submergence. Based on the actual geographic environment and the water level at the waterlogging point, the urban rainstorm-induced submergence algorithm with risk field idea is used to obtain the submergence depth (Fig. 6).

The areas with deeper submergence are mainly located in Futian, Luohu, Bao’an, and Guangming districts, where heavy precipitation is concentrated and the terrain is relatively low, especially in the western and southwestern coastal areas. In addition, the coastal areas may be affected

**Fig. 5** Rainfall and waterlogging point water level on April 11, 2019

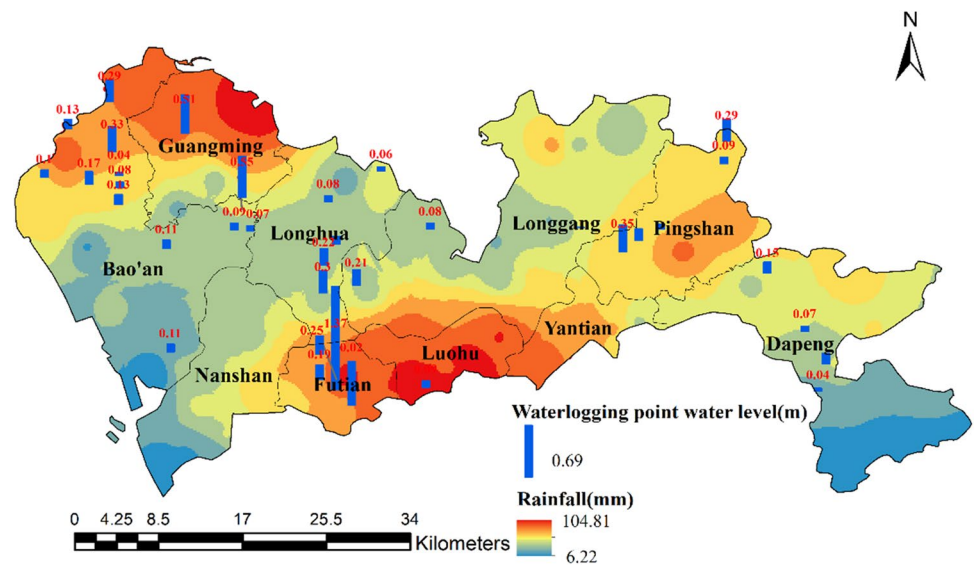
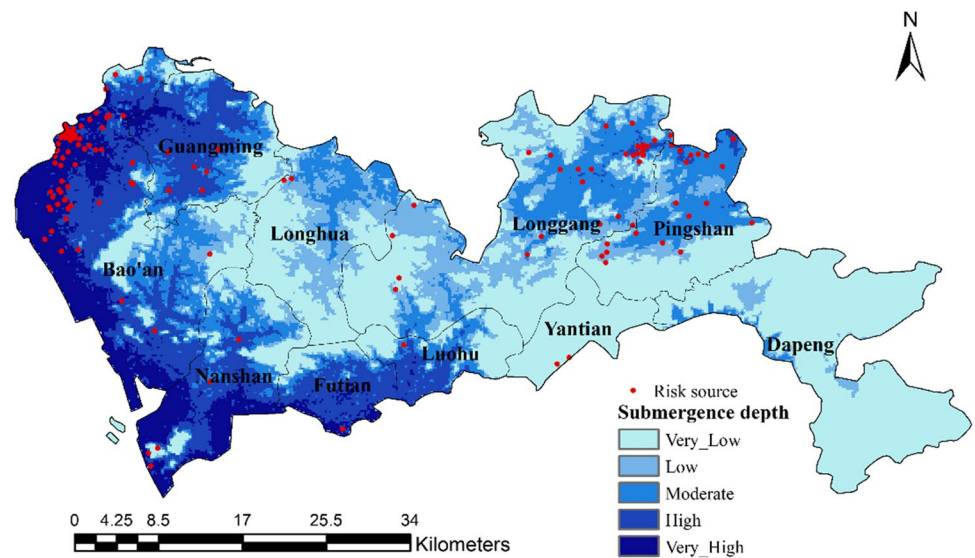


**Fig. 6** Submergence depth on April 11, 2019

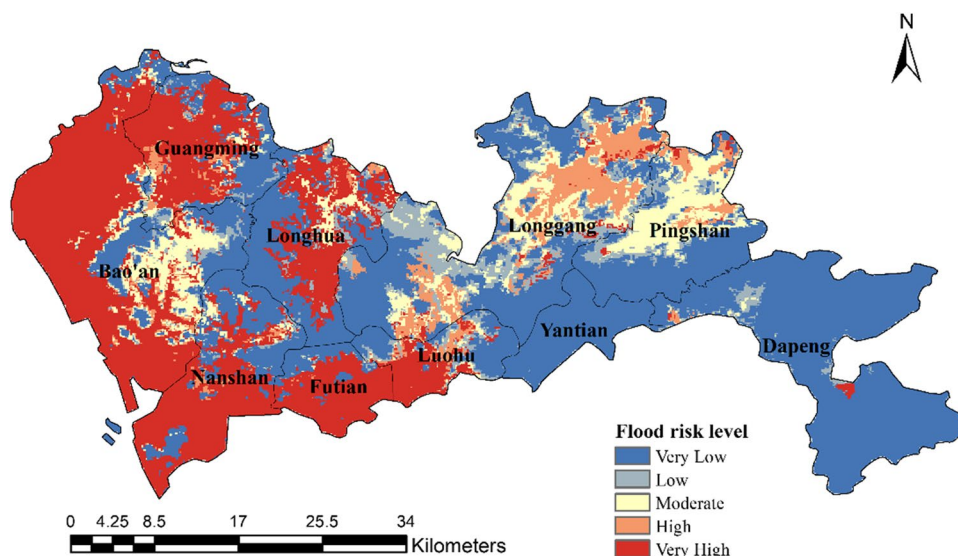


to external tide; submergence is more serious. While some areas in Longhua, Pingshan, and Longgang districts are also submerged, not very deep. Together with the other factor data of flood risk, the flood risk level of each Shenzhen City can be obtained by using the principle of maximum membership (Fig. 7).

It can be seen from Fig. 7 that the very high risk areas are mainly distributed in Futian, Nanshan, Guangming, Bao'an, Luohu, and Longhua districts and some sporadic distribution in Longgang and Pingshan districts and Dapeng New Area. The risk level of most areas in Longgang district is high. The moderate risk level areas are mainly distributed in Pingshan, Longgang, and the central part of Bao'an and Yantian districts; Dapeng New Area, the southern part of Pingshan district, and the eastern part of Longgang district

are low and very low risk level areas. The flood risk map shows that within the percentages of the study area are about 30.93% at very high risk, 6.04% high risk, 9.48% moderate risk, 7.91% low risk, and 45.62% very low risk. In general, the rainstorm-induced flood risk level distribution in Shenzhen is consistent with the submergence depth (Fig. 6). The flood risk level and its causes in different regions are analyzed from the perspective of flood hazard and vulnerability; it is found that the key influencing factors are different in each region, and there are large differences between different regions in each district. For example, Futian, Luohu, and Nanshan districts are the central urban area of Shenzhen, with flat and low topography, adjacent to the seashore, densely populated, economically developed, high proportion of impervious area, and obvious population aging, while

**Fig. 7** Flood risk level distribution on April 11, 2019



these areas have frequent heavy rainfall, external tidal topography, and severe submergence, so the areas are at a very high flood risk level with high flood risk hazard and vulnerability. Other very high and high risk areas also have high hazard and vulnerability, or one of them is very high, such as the western part of Bao'an district has high hazard and vulnerability, Longhua district has high vulnerability, and Longgang district has high hazard. In general, the distribution of rainstorm-induced flood risk level has the characteristics of concentrated contiguous with a high degree of consistency with the submergence situation; the distribution range of very high risk level and very low risk level is large, the areas with high risk level are concentrated in Longgang district, and moderate risk and low risk areas are scattered.

The travel guidelines for rainstorm weather in 2020 were issued by the Transport Bureau of Shenzhen Municipality et al. (2020); there are 128 flood-prone waterlogging points across the city, with relatively dense waterlogging in Futian, Luohu, Nanshan, Guangming, Bao'an, Longhua, and Longgang districts. Compared with the flood risk level map in this paper, the most waterlogging points are located in areas with moderate risk level and above, and the two are basically consistent.

### Flood-induced water pollution risk

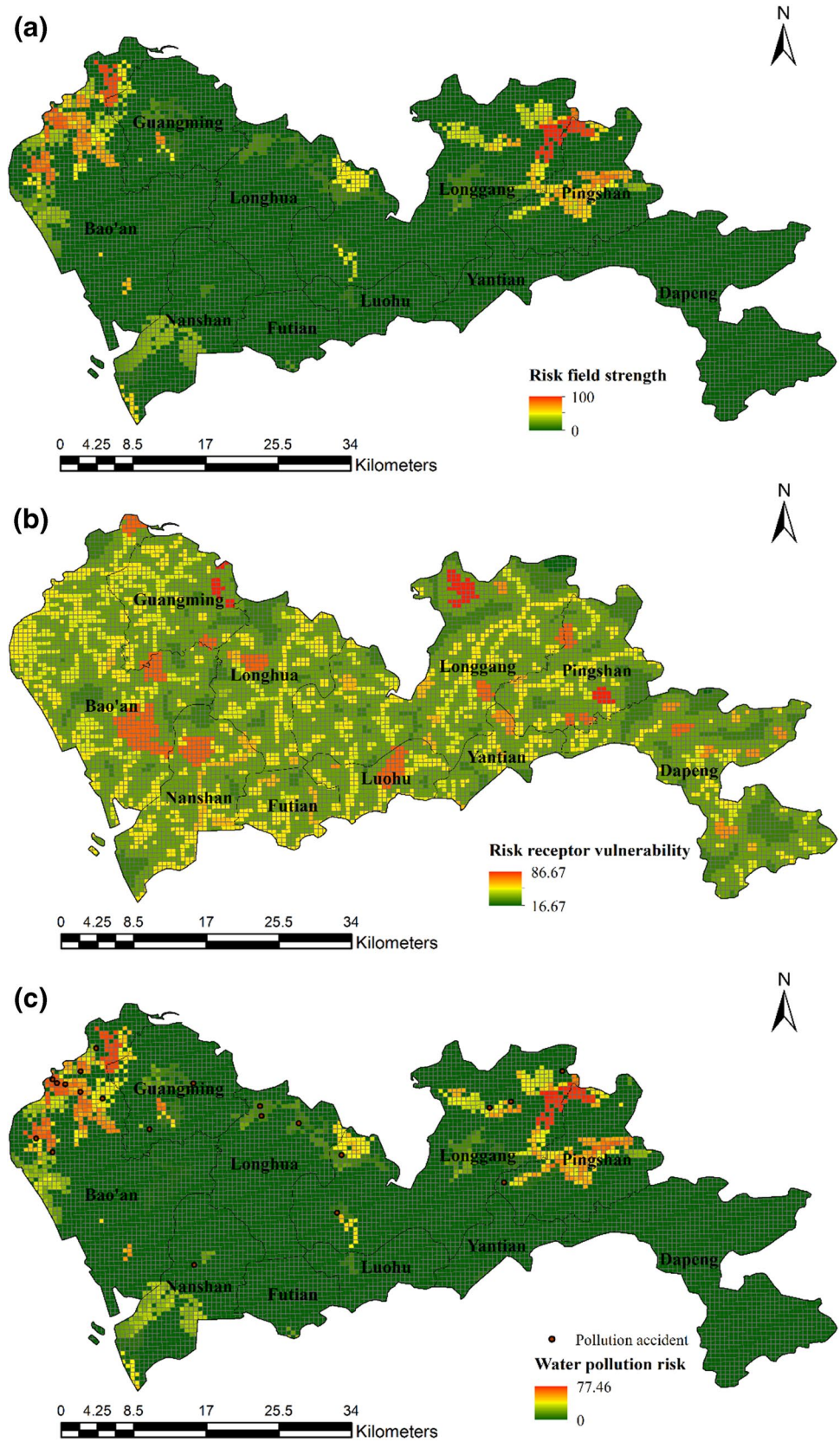
The distribution of flood-induced water pollution risk field strength and water environment receptor vulnerability in Shenzhen are shown in Fig. 8a and b.

In terms of risk field strength distribution, most areas are relatively low, areas with higher risk field strength are mainly distributed in the east of Longgang district, Pingshan and Bao'an districts have some moderate risk field strength

areas, while other areas have low risk field strength, especially in the southern part of Shenzhen. This spatial distribution shows that it is centered on a single or multiple enterprise risk sources with relatively larger and greater risk level, radiating to the outside and gradually decreasing in strength. The area with the highest field strength of flood-induced water pollution risk is located at the eastern junction of Longgang district and Pingshan district, which is affected by the risk sources of more than a dozen risky enterprises nearby; the superposition effect of risk field strength is obvious, and the solid waste treatment plant with the maximum risk source index is also in this area. At the same time, the area often suffers from heavy rainfall, and the submergence is deeper, leading to a high probability of water pollution risk, so the risk field strength of flood-induced water pollution in the region is high. From the distribution of water environment risk receptor vulnerability, the highly sensitive areas are mainly distributed in and around water bodies, especially lakes and reservoirs as water sources, as well as linear areas of rivers.

The results of flood-induced water pollution risk in Shenzhen are calculated after obtaining the field strength of the flood-induced water pollution environmental risk and the vulnerability of the water environment disaster bearing body, and the distribution is shown in Fig. 8c. The most areas are low-risk areas for water pollution, without very high risk areas. Relatively high-risk areas are mainly areas with concentrated risk sources and high flood submergence water depth level, such as the northwest of Bao'an district, the eastern part of Longgang district, and the central part of Pingshan district, where the water environment risk receptor vulnerability values are also relatively high. The area with high risk is 3.14 km<sup>2</sup>, accounting for 0.16% of the study area; the area with moderate risk is 12.8 km<sup>2</sup>, accounting for

**Fig. 8** Spatial distribution of flood-induced water pollution risk analysis in Shenzhen: **a** risk field strength; **b** risk receptors vulnerability; **c** water pollution risk



0.64%, and the area with risk is 297.01 km<sup>2</sup>, accounting for 14.87%. In conclusion, some risk sources are close to water environment sensitive areas, resulting in water environment pollution risk with regional characteristics, and the spatial distribution of water pollution environmental risk is consistent with the distribution of its risk field strength, but the water pollution risk also needs to consider the vulnerability of disaster-bearing body.

The statistics of water pollution accidents in the administrative punishment information released by the Ecology Environment Bureau of Shenzhen Municipality from 2012 to April 2022 are summarized, and the accident statistics of each district (Fig. 9) and the spatial distribution of major water pollution accidents (Fig. 8c) show that the water pollution accidents mainly occur in the western part of Bao'an

district, the eastern part of Longgang district, and the northern part of Longhua district etc., which is basically in line with the spatial distribution result of flood-induced water pollution risks estimated in this paper, indicating that the results in this paper are credible.

### System comprehensive risk

After completing the risk assessment of both flood and water pollution, the two risks are coupled with reference to Table 3 to obtain and draw the system comprehensive risk distribution of rainstorm-induced flood-water pollution in Shenzhen, as shown in Fig. 10 and Table 4.

The areas with very high-high risk are mainly concentrated in the eastern junction of Longgang district and

**Fig. 9** Statistics of water pollution accidents in Shenzhen

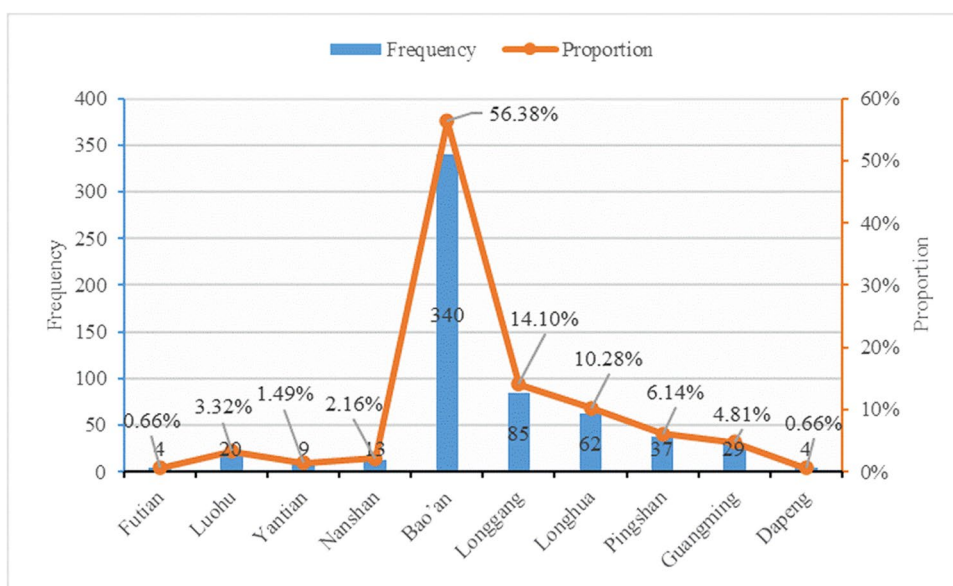


**Fig. 10** System comprehensive risk of rainstorm-induced flood-water pollution in Shenzhen

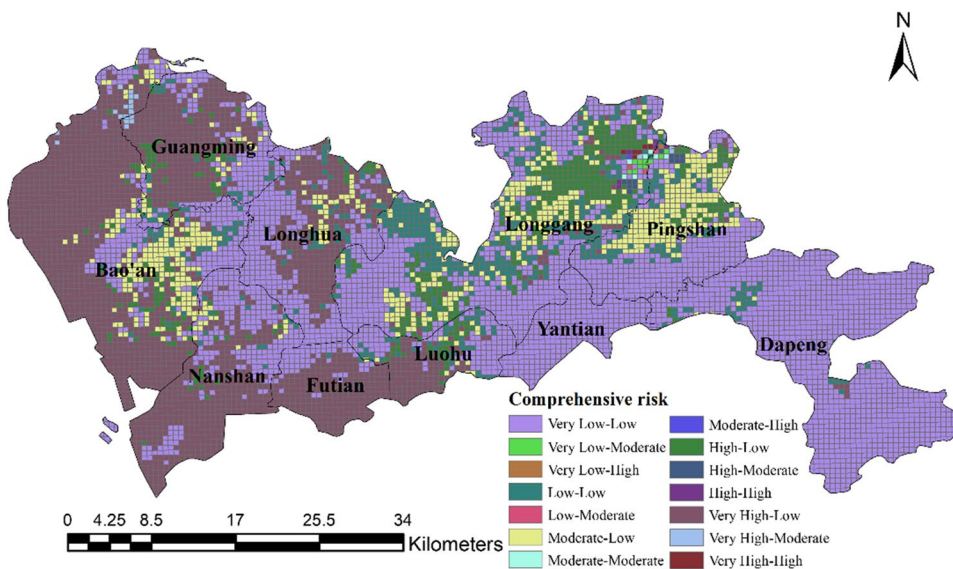


**Table 4** Statistics of the rainstorm-induced flood-water pollution system comprehensive risk zoning area in Shenzhen

Risk level	District (%)										Area km <sup>2</sup>	Percentage %
	Futian	Luohu	Yantian	Nanshan	Bao'an	Longgang	Longhua	Pingshan	Guangming	Dapeng		
Very low-low	22.39	39.95	99.72	35.70	18.00	43.29	46.68	50.86	28.88	95.76	908.67	45.49
Very low-moderate	0.00	0.00	0.00	0.00	0.00	0.46	0.00	0.66	0.00	0.00	2.41	0.12
Very low-high	0.00	0.00	0.00	0.00	0.00	0.00	0.00	0.13	0.00	0.00	0.24	0.01
Low-low	1.19	12.43	0.28	1.65	3.43	20.43	7.13	11.49	5.83	3.25	157.2	7.87
Low-moderate	0.00	0.00	0.00	0.00	0.00	0.17	0.00	0.26	0.00	0.00	0.72	0.04
Moderate-low	0.30	4.23	0.00	2.53	12.46	15.34	5.63	27.21	4.98	0.30	187.63	9.39
Moderate-moderate	0.00	0.00	0.00	0.00	0.00	0.35	0.00	0.26	0.00	0.00	1.69	0.08
Moderate-high	0.00	0.00	0.00	0.00	0.00	0.06	0.00	0.00	0.00	0.00	0.24	0.01
High-low	0.00	9.26	0.00	2.66	3.49	15.63	1.50	6.61	5.97	0.30	116.15	5.81
High-moderate	0.00	0.00	0.00	0.00	0.00	0.35	0.00	0.92	0.00	0.00	3.14	0.16
High-high	0.00	0.00	0.00	0.00	0.00	0.35	0.00	0.40	0.00	0.00	1.45	0.07
Very high-low	76.12	34.13	0.00	57.47	61.77	3.18	39.05	0.92	53.49	0.38	611.66	30.62
Very high-moderate	0.00	0.00	0.00	0.00	0.84	0.06	0.00	0.26	0.85	0.00	4.83	0.24
Very high-high	0.00	0.00	0.00	0.00	0.00	0.35	0.00	0.00	0.00	0.00	1.45	0.07

Pingshan district, accounting for about 0.07% of the total area, because the rainstorm-induced flood risk and flood-induced water pollution risk levels in these areas are relatively high. The area of very high-moderate risk zone is 4.83 km<sup>2</sup>, accounting for 0.24% of the total area. The area of very high-low risk zone is 611.66 km<sup>2</sup>, accounting for 30.62% of the total area, and the detailed percentage of various risk levels in the study area is shown in Table 4. From the system comprehensive risk distribution of each district, Longgang district has very high-high risk areas, accounting for 0.35% of this district. Pingshan district has high-high risk areas, accounting for 0.40% of this district etc. (Table 4). From the distribution of various system comprehensive risk level, the highest percentage is very low-low, followed by very high-low, both accounting for more than 76% of the total area. The areas with very high-high and high-high risk are very small, adding up to only 2.9 km<sup>2</sup>. Figure 10 and Table 4 clearly show that the distribution of various risk levels is characterized by concentrated contiguity, and only a few risk levels are relatively dispersed. Each district contains only a few risk levels, and one or two risk levels account for a relatively high proportion, for example, Longhua district has only five risk levels, of which very low-low and very high-low account for more than 85%.

As mentioned above, the overall system comprehensive risk is mostly very low-low and very high-low, but the rainstorm-induced flood-water pollution risk has chain effect and coupled superposition effect, so city managers need to pay attention to areas with frequent natural disaster risks; dense distribution of risk source enterprises and better water quality have high risk. Furthermore, it should be noted that there are few regions with relatively high risk for both disasters, and a relatively high percentage of areas with high risk level for one hazard, covering approximately 617.94 km<sup>2</sup> and accounting for 30.93% of the total area, which requires the attention of managers.

## Discussion

The existing disaster risk assessment methods rarely focus on how risk factors are released, the spatial distribution pattern after release, and how risk receptors are exposed to risk factors and the degree of damage, which cannot describe the risk occurrence and development process well. These problems can be better explained and analyzed by the risk field model. When analyzing the rainstorm-induced flood risk, some existing methods, such as the SCS-CN model and the isometric method, can quickly obtain the submergence results, but their prerequisite assumptions of uniform precipitation on the regional surface, flat terrain, less research on large-scale areas, and no consideration of connectivity (Nagarajan and Poongothai 2012). This paper uses the risk

field algorithm to obtain the submergence depth and range, which has two advantages. On the one hand, it can clearly describe the process of rainstorm-induced submergence in urban areas. On the other hand, in the current general lack of data, the algorithm proposed in this paper can use limited data to quickly determine the submergence depth and range, although it is not as accurate as the hydraulic and hydrological models; its calculation is simple and practical and does not require a large number of high-precision data that is difficult to obtain (Beven 2019; Song et al. 2015). Urban flood-induced water pollution risk assessment using risk field theory fully considers the hazard of risk sources and the vulnerability of risk receptors, as well as the spatial location relationship between them; grids the area; and visualizes the risk on the map. This method can well characterize the water pollution risk characteristics and comprehensively understand the distribution, type, and scale of regional water pollution risk. Moreover, most of the current studies take administrative regions as the study units, and the microscale is less raster-based, so the variability of the results cannot be well reflected.

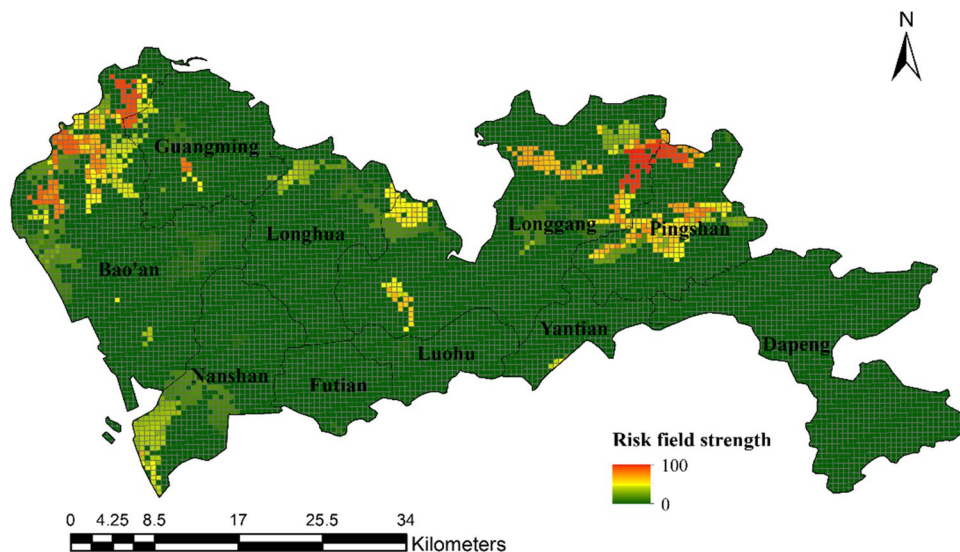
The research on the disaster chain assumes that the chain relationship is certain to occur and does not involve the possibility of inducing accidents. In this paper, the risk field strength formula is improved by increasing the likelihood of emergencies based on Bayesian conditional probability, and comparing the risk field strength of flood-induced water pollution (Fig. 8a) and sudden water environmental pollution (Fig. 11), it is found that the relative risk value of flood-induced water pollution risk field strength in 70.24% of the grids has been reduced, indicating that flood and water pollution became less likely to occur simultaneously, which is more in line with the actual situation. However, flood disasters in urban areas increase the frequency of water pollution, and if flood and water pollution jointly affect a certain area,

the risk of these two disasters is coupled and superimposed, exacerbating the hazard and causing more serious harm once they occur simultaneously.

The scale of data is spatiotemporal, and dividing the study area into several evaluation units is an important way to achieve risk assessment and draw risk maps (Zhao 2012), but there is currently no unified standard or method to determine the spatial scale of evaluation units. In the specific analysis, the size of the evaluation unit spatial scale can be confirmed according to the scope of the study area, the scale of the data, etc., or referring to the previous experience and research results (Zhao 2016), and further research is needed to quantify how to ensure a reasonable and scientific grid scale. In this paper, the grid method can better reflect the spatial distribution characteristics of regional environmental risk, accurately identify high-risk areas, while seeking accurate and high-resolution data as much as possible to improve the accuracy of risk assessment results, although this may reduce some computational efficiency, so the study based on advanced methods to collect more and more high-resolution data while also considering the stability and computational efficiency of the algorithm. The research results accurately identify high-risk areas, provide accurate reference for predicting and managing regional environmental risk, help relevant departments change from passive environmental risk emergency management to active risk management, and timely identify and solve the problems existing in environmental risk areas.

In the paper, the influence of ground facilities such as buildings on ponding diffusion is not considered when analyzing submergence depth. The risk field strength calculation utilizes the Q value, without using the actual water environment risk material discharge. These may lead to some uncertainty in the results that require further research to solve. In the future, it is also necessary to study the chain effect

**Fig. 11** Risk field strength of sudden water pollution



and coupled superposition effect of chain-field combination; further explore other disasters induced by flood; extend the disaster chain; and more importantly, explore a universally applicable multi-hazard risk coupling evaluation method, so as to comprehensively study the urban flood-induced systematic risk.

## Conclusion

The study proposes a novel spatial framework for the rainstorm-induced flood-water pollution system comprehensive risk based on fuzzy comprehensive evaluation method, Bayesian network, and risk field theory. Firstly, the submergence depth calculated by the risk field idea algorithm is combined with other influencing factors to obtain the flood risk distribution by using the fuzzy comprehensive evaluation method. Secondly, the possibility of flood-induced water pollution determined by the conditional probability of Bayesian theory is added to improve the gridded environmental risk analysis method to assess the environmental risk of flood-induced water pollution. Finally, the [flood-pollution] risk level matrix is constructed to explore the rainstorm-induced flood-water pollution system comprehensive risk in Shenzhen.

The established model is applied to evaluate the rainstorm-induced flood-water pollution system comprehensive risk in Shenzhen, and the results show that there is no very high-very high systematic risk level area. The eastern junction of Longgang district and Pingshan district has high-high and above risk level areas, only 2.9 km<sup>2</sup>; where the rainstorm-induced flood risk is very high, the probability of flood-induced water pollution is also high, and the concentration of risk sources as well as the vulnerability value of water environment risk receptors is also relatively high. The risk level in most areas is very low-low and very high-low, accounting for more than 76% of the study area. The rainstorm-induced flood-water pollution risk has a chain effect and coupled superposition effect; the area with very high flood risk accounts for 30.93% of the total area, about 617.94 km<sup>2</sup>, and special attention should be paid if the risk source is in this area.

The research has achieved some innovative results, such as using risk field theory to assess the risk of various disasters, quantitatively analyzing the induced chain relationship based on Bayesian network, improving the environmental risk field calculation method, and characterizing the systemic risk of induced multi-hazard by drawing on the risk matrix. The research results provide a scientific basis for formulating urban planning policies, flood control, and ecological environment management. The rainstorm-induced system comprehensive risk can be mitigated and reduced by taking a series of engineering and non-engineering

measures to cut off the transmission of chain risk and eliminate subsequent risks in the chain. Specific strategies include strengthening the rainstorm forecast, optimizing industrial layout, improving access standards, enhancing source prevention and control, monitoring and early warning, developing targeted emergency plans, implementing hierarchical management, and introducing insurance system in the future to hedge environmental pollution risks.

**Supplementary Information** The online version contains supplementary material available at <https://doi.org/10.1007/s11356-023-26762-3>.

**Acknowledgements** The authors would like to express our gratitude to the Ecology Environment Bureau of Shenzhen Municipality for their data support. All the anonymous reviewers are appreciated for their valuable and constructive comments which have improved the quality of the paper.

**Author contribution** Huang Shanqing: conceptualization, methodology, software, analysis, visualization, writing — original draft. Wang Huimin: conceptualization, supervision, writing — review and editing. Liu Gaofeng: conceptualization, methodology, supervision, writing — review and editing. Huang Jing: writing — review and editing, Supervision. Zhu Jindi: data curation, writing — review and editing.

**Funding** The work was supported by the National Natural Science Foundation of China (Grant No. 72174054, Grant No. 91846203, Grant No. 42171081).

**Data availability** Data will be made available on request.

## Declarations

**Ethical approval** Not applicable.

**Consent to participate** Not applicable.

**Consent for publication** Not applicable.

**Competing interests** The authors declare no competing interests.

## References

- Abdalla R, Elawad Y, Chen Z, Han SS, Xia R (2014) A GIS-supported fuzzy-set approach for flood risk assessment. *Can Water Resour J* 39(1):3–14. <https://doi.org/10.1080/07011784.2014.881058>
- Albanese S, De Vivo B, Lima A, Frattasio G, Kribek B, Nyambe I, Majer V (2014) Prioritising environmental risk at the regional scale by a GIS aided technique: the Zambian Copperbelt Province case study. *J Geochem Explor* 144:433–442. <https://doi.org/10.1016/j.gexplo.2014.03.014>
- Alvarez-Galvez J (2016) Discovering complex interrelationships between socioeconomic status and health in Europe: a case study applying Bayesian Networks. *Soc Sci Res* 56:133–143. <https://doi.org/10.1016/j.ssresearch.2015.12.011>
- Andric JM, Lu D-G (2016) Risk assessment of bridges under multiple hazards in operation period. *Saf Sci* 83:80–92. <https://doi.org/10.1016/j.ssci.2015.11.001>
- Antonioni G, Landucci G, Necci A, Gheorghiu D, Cozzani V (2015) Quantitative assessment of risk due to NaTech scenarios caused



- by floods. *Reliab Eng Syst Saf* 142:334–345. <https://doi.org/10.1016/j.res.2015.05.020>
- Arnell NW, Gosling SN (2016) The impacts of climate change on river flood risk at the global scale. *Clim Change* 134(3):387–401. <https://doi.org/10.1007/s10584-014-1084-5>
- Benito G, Lang M, Barriendos M, Llasat MC, Frances F, Ouarda T, Thorndycraft VR, Enzel Y, Bardossy A, Coeur D, Bobee B (2004) Use of systematic, palaeoflood and historical data for the improvement of flood risk estimation. Review of scientific methods. *Nat Hazards* 31(3):623–643
- Bevacqua E, Voudoukas MI, Shepherd TG, Vrac M (2020) Brief communication: the role of using precipitation or river discharge data when assessing global coastal compound flooding. *Nat Hazards Earth Sys Sci* 20(6):1765–1782. <https://doi.org/10.5194/nhess-20-1765-2020>
- Beven K (2019) How to make advances in hydrological modelling. *Hydrol Res* 50(6):1481–1494. <https://doi.org/10.2166/nh.2019.134>
- Boenne W, Desmet N, Van Looy S, Seuntjens P (2014) Use of online water quality monitoring for assessing the effects of WWTP overflows in rivers. *Environ Sci-Process Impacts* 16(6):1510–1518. <https://doi.org/10.1039/c3em00449j>
- Cai T, Li X, Ding X, Wang J, Zhan J (2019) Flood risk assessment based on hydrodynamic model and fuzzy comprehensive evaluation with GIS technique. *Int J Disast Risk Reduct* 35. <https://doi.org/10.1016/j.ijdr.2019.101077>
- Cao G, Gao Y, Wang J, Zhou X, Bi J, Ma Z (2019) Spatially resolved risk assessment of environmental incidents in China. *J Clean Prod* 219:856–864. <https://doi.org/10.1016/j.jclepro.2019.02.130>
- Chen Y, Zhou H, Zhang H, Du G, Zhou J (2015) Urban flood risk warning under rapid urbanization. *Environ Res* 139:3–10. <https://doi.org/10.1016/j.envres.2015.02.028>
- Chen HX, Zhang S, Peng M, Zhang LM (2016) A physically-based multi-hazard risk assessment platform for regional rainfall-induced slope failures and debris flows. *Eng Geol* 203:15–29. <https://doi.org/10.1016/j.enggeo.2015.12.009>
- Chen W, Huang G, Zhang H, Wang W (2018) Urban inundation response to rainstorm patterns with a coupled hydrodynamic model: a case study in Haidian Island, China. *J Hydrol* 564:1022–1035. <https://doi.org/10.1016/j.jhydrol.2018.07.069>
- Cozzani V, Campedel M, Renni E, Krausmann E (2010) Industrial accidents triggered by flood events: analysis of past accidents. *J Hazard Mater* 175(1–3):501–509. <https://doi.org/10.1016/j.jhazmat.2009.10.033>
- Cozzani V, Antonioni G, Landucci G, Tugnoli A, Bonvicini S, Spadoni G (2014) Quantitative assessment of domino and NaTech scenarios in complex industrial areas. *J Loss Prev Process Ind* 28:10–22. <https://doi.org/10.1016/j.jlpi.2013.07.009>
- Geng Y, Dai E, Wang G, Jin Z, Zhang J (2022) Spatio-temporal distribution, evolution and influence mechanism of water pollution incidents in China. *Environ Pollut Control* 44(3):413–419. <https://doi.org/10.15985/j.cnki.1001-3865.2022.03.023>. (in Chinese)
- Gill JC, Malamud BD (2016) Hazard interactions and interaction networks (cascades) within multi-hazard methodologies. *Earth Syst Dynam* 7(3):659–679. <https://doi.org/10.5194/esd-7-659-2016>
- Guan X, Ren X, Tao Y, Chang X, Li B (2022) Study of the water environment risk assessment of the upper reaches of the Baiyangdian Lake, China. *Water* 14(16). <https://doi.org/10.3390/w14162557>
- Hadipour V, Vafaie F, Deilami K (2020) Coastal flooding risk assessment using a GIS-based spatial multi-criteria decision analysis approach. *Water* 12(9). <https://doi.org/10.3390/w12092379>
- Han L, Song YH, Duan L, Yuan P (2015) Risk assessment methodology for Shenyang Chemical Industrial Park based on fuzzy comprehensive evaluation. *Environ Earth Sci* 73(9):5185–5192. <https://doi.org/10.1007/s12665-015-4324-8>
- Huang G, Li B (2021) Risk assessment of storm water flooding in Shenzhen City based on fuzzy comprehensive evaluation method. *J Water Resour Water Eng* 32(1):1–6. <https://doi.org/10.11705/j.issn.1672-643X.2021.01.01>. (in Chinese)
- Huang L, Wan W, Li F, Li B, Yang J, Bi J (2011) A two-scale system to identify environmental risk of chemical industry clusters. *J Hazard Mater* 186(1):247–255. <https://doi.org/10.1016/j.jhazmat.2010.10.117>
- Huang W, Shuai B, Zhang R, Xu M, Xu Y, Yu Y, Antwi E (2020) A new system risk definition and system risk analysis approach based on improved risk field. *Ieee Trans Reliab* 69(4):1437–1452. <https://doi.org/10.1109/tr.2019.2942373>
- Huang S, Wang H, Xu Y, She J, Huang J (2021) Key disaster-causing factors chains on urban flood risk based on bayesian network. *Land* 10(2). <https://doi.org/10.3390/land10020210>
- Jato-Espino D, Lobo A, Ascorbe-Salcedo A (2019) Urban flood risk mapping using an optimised additive weighting methodology based on open data. *J Flood Risk Manag* 12(S1). <https://doi.org/10.1111/jfr3.12533>
- Jiang Y, Zevenbergen C, Ma Y (2018) Urban pluvial flooding and stormwater management: a contemporary review of China's challenges and “sponge cities” strategy. *Environ Sci Policy* 80:132–143. <https://doi.org/10.1016/j.envsci.2017.11.016>
- Johnson K, Depietri Y, Breil M (2016) Multi-hazard risk assessment of two Hong Kong districts. *Int J Disast Risk Reduct* 19:311–323. <https://doi.org/10.1016/j.ijdr.2016.08.023>
- Kappes MS, Papatoma-Koehle M, Keiler M (2012) Assessing physical vulnerability for multi-hazards using an indicator-based methodology. *Appl Geogr* 32(2):577–590. <https://doi.org/10.1016/j.apgeog.2011.07.002>
- Karatzetou A, Stefanidis S, Stefanidou S, Tsinidis G, Pitilakis D (2022) Unified hazard models for risk assessment of transportation networks in a multi-hazard environment. *Int J Disast Risk Reduct* 75:102960. <https://doi.org/10.1016/j.ijdr.2022.102960>
- Karatzetou A, Stefanidou S, Stefanidis S, Tsinidis G, Pitilakis D (2021) Towards a unified seismic- flood hazard model for risk assessment of roadway networks in Greece. 8th International Conference on Computational Methods in Structural Dynamics and Earthquake Engineering Methods in Structural Dynamics and Earthquake Engineering, Athens, Greece. <https://doi.org/10.7712/120121.8730.19588>
- Khakzad N, Van Gelder P (2018) Vulnerability of industrial plants to flood-induced natechs: a Bayesian network approach. *Reliab Eng Syst Saf* 169:403–411. <https://doi.org/10.1016/j.res.2017.09.016>
- Krausmann E, Cruz AM (2013) Impact of the 11 March 2011, Great East Japan earthquake and tsunami on the chemical industry. *Nat Hazards* 67(2):811–828. <https://doi.org/10.1007/s11069-013-0607-0>
- Krausmann E, Cozzani V, Salzano E, Renni E (2011) Industrial accidents triggered by natural hazards: an emerging risk issue. *Nat Hazards Earth Sys Sci* 11(3):921–929. <https://doi.org/10.5194/nhess-11-921-2011>
- Krishnakumar A, Jose J, Kaliraj S, Aditya SK, Krishnan KA (2022) Assessment of the impact of flood on groundwater hydrochemistry and its suitability for drinking and irrigation in the River Periyar Lower Basin, India. *Environ Sci Pollut Res* 29(19):28267–28306. <https://doi.org/10.1007/s11356-021-17596-y>
- Lai C, Chen X, Wang Z, Yu H, Bai X (2020) Flood risk assessment and regionalization from past and future perspectives at basin scale. *Risk Anal* 40(7):1399–1417. <https://doi.org/10.1111/risa.13493>
- Li L, Xu T, Chen Y (2016) Improved urban flooding mapping from remote sensing images using generalized regression neural network-based super-resolution algorithm. *Remote Sens* 8(8). <https://doi.org/10.3390/rs8080625>
- Lian J, Xu H, Xu K, Ma C (2017) Optimal management of the flooding risk caused by the joint occurrence of extreme rainfall and high tide

- level in a coastal city. *Nat Hazards* 89(1):183–200. <https://doi.org/10.1007/s11069-017-2958-4>
- Link O, Brox-Escudero LM, Gonzalez J, Aguayo M, Torrejon F, Montalva G, Eguibar-Galan MA (2019) A paleo-hydro-geomorphological perspective on urban flood risk assessment. *Hydrol Process* 33(25):3169–3183. <https://doi.org/10.1002/hyp.13590>
- Liu YH, Fang PP, Bian DD, Zhang HW, Wang SX (2014) Fuzzy comprehensive evaluation for the motion performance of autonomous underwater vehicles. *Ocean Eng* 88:568–577. <https://doi.org/10.1016/j.oceaneng.2014.03.013>
- Liu RZ, Zhang K, Zhang ZJ, Borthwick AGL (2018) Watershed-scale environmental risk assessment of accidental water pollution: the Case of Laoguan River, China. *J Environ Inform* 31(2):87–96. <https://doi.org/10.3808/jei.201600346>
- MEP (2018a) Risk classification method of environmental incidents in enterprises (in Chinese). MEP, China
- MEP (2018b) Recommended methods for risk assessment of environmental incidents in administrative areas (in Chinese). MEP, China
- Muis S, Guneralp B, Jongman B, Aerts J, Ward PJ (2015) Flood risk and adaptation strategies under climate change and urban expansion: a probabilistic analysis using global data. *Sci Total Environ* 538:445–457. <https://doi.org/10.1016/j.scitotenv.2015.08.068>
- Mukhopadhyay A, Hazra S, Mitra D, Hutton C, Chanda A, Mukherjee S (2016) Characterizing the multi-risk with respect to plausible natural hazards in the Balasore coast, Odisha, India: a multi-criteria analysis (MCA) appraisal. *Nat Hazards* 80(3):1495–1513. <https://doi.org/10.1007/s11069-015-2035-9>
- Nagarajan N, Poongothai S (2012) Spatial mapping of runoff from a watershed using SCS-CN method with remote sensing and GIS. *J Hydrol Eng* 17(11):1268–1277. [https://doi.org/10.1061/\(asce\)he.1943-5584.0000520](https://doi.org/10.1061/(asce)he.1943-5584.0000520)
- Qiu WH, Sun J, Fang MJ, Luo SS, Tian YQ, Dong PY, Xu BT, Zheng CM (2019) Occurrence of antibiotics in the main rivers of Shenzhen, China: association with antibiotic resistance genes and microbial community. *Sci Total Environ* 653:334–341. <https://doi.org/10.1016/j.scitotenv.2018.10.398>
- Sarica GM, Zhu T, Jian W, Lo EY-M, Pan T-C (2021) Spatio-temporal dynamics of flood exposure in Shenzhen from present to future. *Env Plan B-Urban Anal City Sci* 48(5):1011–1024. <https://doi.org/10.1177/2399808321991540>
- Schumann GJP, Andreadis KM (2016) A method to assess localized impact of better floodplain topography on flood risk prediction. *Adv Meteorol* 2016. <https://doi.org/10.1155/2016/6408319>
- Shadmehri Toosi A, Calbimonte GH, Nouri H, Alaghmand S (2019) River basin-scale flood hazard assessment using a modified multi-criteria decision analysis approach: a case study. *J Hydrol* 574:660–671. <https://doi.org/10.1016/j.jhydrol.2019.04.072>
- Shao Z, Wu W, Li D (2021) Spatio-temporal-spectral observation model for urban remote sensing. *Geo-Spat Inf Sci* 24(3):372–386. <https://doi.org/10.1080/10095020.2020.1864232>
- Song C, Wang H, Tang D (2015) Research progress and development trend of storm water management model. *China Water Wastewater* 31(16):16–20. <https://doi.org/10.19853/j.zgjsps.1000-4602.2015.16.005>. (in Chinese)
- Sun N, Hall M, Hong B, Zhang L (2014) Impact of SWMM catchment discretization: case study in Syracuse. *New York J Hydrol Eng* 19(1):223–234. [https://doi.org/10.1061/\(asce\)he.1943-5584.0000777](https://doi.org/10.1061/(asce)he.1943-5584.0000777)
- Tesfamariam S, Sadiq R (2006) Risk-based environmental decision-making using fuzzy analytic hierarchy process (F-AHP). *Stoch Environ Res Risk Assess* 21(1):35–50. <https://doi.org/10.1007/s00477-006-0042-9>
- Transport Bureau of Shenzhen Municipality, Meteorological Bureau of Shenzhen Municipality, Emergency Management Bureau of Shenzhen Municipality (2020) Travel guidelines for rainstorm weather in Shenzhen (in Chinese). [http://jtyz.sz.gov.cn/zwgk/jttx/cxtx/content/post\\_8817277.html](http://jtyz.sz.gov.cn/zwgk/jttx/cxtx/content/post_8817277.html). Accessed 21 January 2022
- Wu WY, Westra S, Leonard M (2021) Estimating the probability of compound floods in estuarine regions. *Hydrol Earth Syst Sci* 25(5):2821–2841. <https://doi.org/10.5194/hess-25-2821-2021>
- Xing Y, Wang X, Ke X, Wu T, Teng W (2016) Method of regional acute environmental risk assessment based on risk field. *China Environ Sci* 36(4):1268–1274 (in Chinese)
- Yang H, Liu B, Huang J (2018) Forecast model parameters calibration method for sudden water pollution accidents based on improved Bayesian-Markov chain Monte Carlo. *Control Decis* 33(4):679–686. <https://doi.org/10.13195/j.kzyjc.2017.0213>. (in Chinese)
- Yin J, Ye M, Yin Z, Xu S (2015) A review of advances in urban flood risk analysis over China. *Stoch Environ Res Risk Assess* 29(3):1063–1070. <https://doi.org/10.1007/s00477-014-0939-7>
- Zadeh LA (1965) Fuzzy sets. *Inf Control* 8(3):338–353. [https://doi.org/10.1016/S0019-9958\(65\)90241-X](https://doi.org/10.1016/S0019-9958(65)90241-X)
- Zhang H, Cheng X, Jin L, Zhao D, Feng T, Zheng K (2020a) A method for dynamical sub-watershed delimitating by no-fill digital elevation model and defined precipitation: a case study of Wuhan, China. *Water* 12(2). <https://doi.org/10.3390/w12020486>
- Zhang H, Li W, Miao P, Sun B, Kong F (2020b) Risk grade assessment of sudden water pollution based on analytic hierarchy process and fuzzy comprehensive evaluation. *Environ Sci Pollut Res* 27(1):469–481. <https://doi.org/10.1007/s11356-019-06517-9>
- Zhang Y, Li Z, Ge W, Wang J, Guo X, Wang T, Zhang H (2022) Evaluation of the water pollution risk of dam and dike-break floods in the inundated area. *Environ Sci Pollut Res* 29(50):76365–76377. <https://doi.org/10.1007/s11356-022-20742-9>
- Zhao S (2012) A preliminary study on the spatial and temporal scales of natural disaster risk analysis. *J Catastrophol* 27(2):1–6+18+7 (in Chinese)
- Zhao S (2016) Secondary discussion on spatial-and-temporal scale of natural disaster risk. *J Catastrophol* 31(4):1–10. <https://doi.org/10.3969/j.issn.1000-811X.2016.04.001>. (in Chinese)
- Zhao G, Pang B, Xu ZX, Peng DZ, Xu LY (2019) Assessment of urban flood susceptibility using semi-supervised machine learning model. *Sci Total Environ* 659:940–949. <https://doi.org/10.1016/j.scitotenv.2018.12.217>
- Zhou X, Cao G, Yu F, Liu Q, Ma G, Yang W (2020a) Risk zoning of acute water pollution in the Yangtze River Economic Belt. *Acta Sci Circum* 40(1):334–342. <https://doi.org/10.13671/j.hjkxxb.2019.0369>. (in Chinese)
- Zhou X, Yu F, Liu Q, Cao G, Ma G, Yang W (2020b) Risk zoning of sudden water pollution in Dongjiang River basin. *Acta Ecol Sin* 40(14):4813–4822. <https://doi.org/10.5846/stxb201905090943>. (in Chinese)

**Publisher's note** Springer Nature remains neutral with regard to jurisdictional claims in published maps and institutional affiliations.

Springer Nature or its licensor (e.g. a society or other partner) holds exclusive rights to this article under a publishing agreement with the author(s) or other rightsholder(s); author self-archiving of the accepted manuscript version of this article is solely governed by the terms of such publishing agreement and applicable law.